Evaluation of the efficiency of (gypsum-lime) concrete used in the roofs of Mohamed Ali family buildings (1880 – 1900) and its impact on the preservation state of ceiling decorations

Gamal Saad [1], Mohamed Hawash [2], Osama Ahmed [3], Musa Babiker [4], Khaled Zid [5]

[1,3,4, -] Civil and Architectural Engineering Department ,College of Engineering and Computer Science, Jazan University, Kingdom of Saudi Arabia.
[2-] Department of restoration, faculty of archaeology, Cairo University, Egypt.
[5-] Civil and Architectural Engineering Department ,College of Engineering and Computer Science, Jazan University, Kingdom of Saudi Arabia.& Architectural Engineering Department, College of Engineering, Helwan University, Egypt.

Abstract:
Egypt   have a wealth of heritage and archaeological buildings from prehistoric until the era of the Muhammad Ali family (1805 - 1952), where European influences prevailed in this period, mixed with traditional Islamic styles. Our building in this paper is a tomb dating back to the family of Ismail Sidqi Pasha (1875 - 1950). This building was built before   1900, as the first tombstone dates to 1900,   therefore   it was built in the period between 1880 and 1900. The roof of the building is considered one of the most building elements   vulnerable to damage due to rainwater that accumulates on the roof for a long time in winter,   beside   insulation material damage, causing Lots of damage to the roof. Consequently, it affected the ceiling decorations. It is known that during the construction of the ceiling, the use of cement as a building material began to spread,   the ceiling   was implemented by placing iron beams and filling between the beams with a material of the unreinforced concrete, so damages to the ceiling were studied, Such as the loss of render layers , the salts efflorescence   and colors deterioration and loss. The components of the unreinforced concrete used in the ceiling were studied, which was completely devoid of cement and consisted mainly of gypsum, lime, and gravel of limestone and basalt. In studying the components of concrete, the X-ray diffraction XRD method was used to identify the minerals that represent concrete binder. Scanning electron microscope SEM with EDX used to identify fillers (stone gravel – sand) and explain the damage processes of concrete. Samples were built with the same concrete components to carry out mechanical tests such as compression tests and to determine physical properties such as density and porosity. A simulation model was built identical to Roof slab, where a concrete model was implemented between the two edges of the iron beams the mock-up tested to determine its ability to bear loads by performing a bending test, which gave acceptable results for this composition of concrete (gypsum + lime). As a result of tests and analyses it was found that the high percentage of porosity of the concrete was a reason for the transmission of water and This led to the spread of salts within concrete matrix and on the surface of the colors and render, exposure to water and salt damage reducing the mechanical properties of the concrete by half. and this led to the occurrence of Damages to the ceiling like falling of render layers, exfoliation of colors, , and   salts efflorescence
Keywords:
Concrete (gypsum - lime), unreinforced concrete, gravel concrete, renders, salts, compression test, bending test, roof simulation model (mock-up)

I.   INTRODUCTION:
The family of Ismail Sedqi Pasha, build up vault, Ismail Sedqi Pasha an Egyptian politician who assumed the prime minister   of Egypt in 1930 during the reign of King Fouad I. He served as prime minister for a second time on 1946. [1] Another family share this grave with Ismail Sedqi Pasha family , according to the National Apparatus for Cultural Coordination. They are the family Amin Pasha Sidi Ahmed and the family of Ismail Sedqi Pasha. The burial site is registered under No. 0424000259 in the National Apparatus for Urban Coordination decree No. 233 of 2023 [2]   The cemetery is located in the Imam Al-Shafi'i and Imam Al-Laith areas in Cairo Governorate .

Description of the building

The building is a large burial chamber containing 6 graves. Each grave has a gilded marble composition. The area of the building is 85.5 m2, and its dimensions are 9 x 9.5 m. The height of the building is 10 m. The main entrance is located on the north side with a door measuring 3 m high and 160 cm wide. Its fillings are made in the shape of a plate. Al-Najmi (Islamic decorative design) . Around the door is a window on the right side. It is 2.5 meters high and 1 meter wide. Its fillings are made in the shape of Al-Maqali (Islamic decorative design). There is a similar window on the left side, and on each of the other facades of the building there are three windows. Similar wooden windows in tha main façade , at the top of each, there are twin windows made of stucco windows covered with glass, surmounted by a A circle-shaped stucco windows covered with glass with a muqarnas (Islamic decorative design) cornice at the top. Image (1)
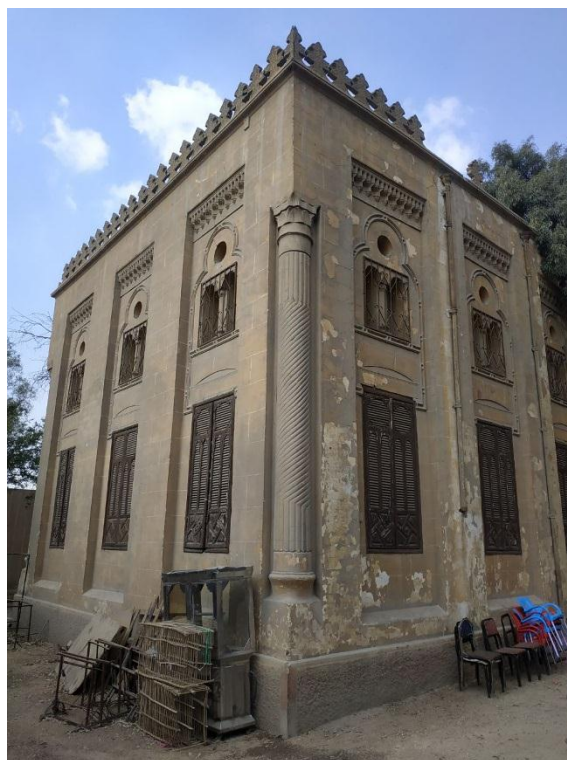

Image (1) Shows the vault building from the outside

On top of the building, there are artificial stone formation in the form of Islamic decorations surrounding the building from the top. Inside the building walls are decorated with modified floral decorations (Islamic style) and the walls and ceiling were painted with oil colors.

The ceiling is the subject of study

The method of implementing roofs in some buildings of the Muhammad Ali family was an imitation of the method of roofing with wooden beams by using iron beams instead of wooden beams, and they were distributed over the entire surface of the roof with spaces between them from 50 to 60 cm. In case that the length of the space exceeded 5 m, tensioners were made. In the middle of the iron beams to connect them together from the middle so that there was no deflection of the beams, and the space between each beam and the other was filled with cement concrete or white concrete so that this concrete entered the C-shaped cavity in the iron beams. [3] The ceiling here is filled with white concrete. Image (2 ,3)

Image (2) show Iron beams on top of the building

Image (3) show Iron beams from inside the building

Over many years, the roof   exposed to rainwater, which was not drained from the top of the roof, but was absorbed by the roof slab due to   the insulation layer damage on top of the roof. The presence of water has some negative effects, such as The cracks spread parallel to the path of the steel beams , rusting of iron beams, separation of render layers, peeling of colors, and falling parts of concrete that fills   between the iron beams. Image (4,5,6,7,8,9) Figure (1,2)

The wet state in which polluted gases turn into acids, for example carbon dioxide present in the atmosphere or produced by various industries, which is deposited on the roofs of ancient buildings that have absorbed large quantities of this water and dissolves in water and turns into carbonic acid. This weak acid is responsible for dissolving and disintegrating Layers of concrete, render and colors. [4]

The   salt presence increases with the presence of moisture, as the formation of salt depends on two factors: first, the degree of solubility of the salt, and second, the ability to transfer salt to building materials and the porosity of building materials. [5] The porosity rate of the concrete is 34%, and the salt present is halite with a high degree of solubility. The damaged parts were used as samples for the study.
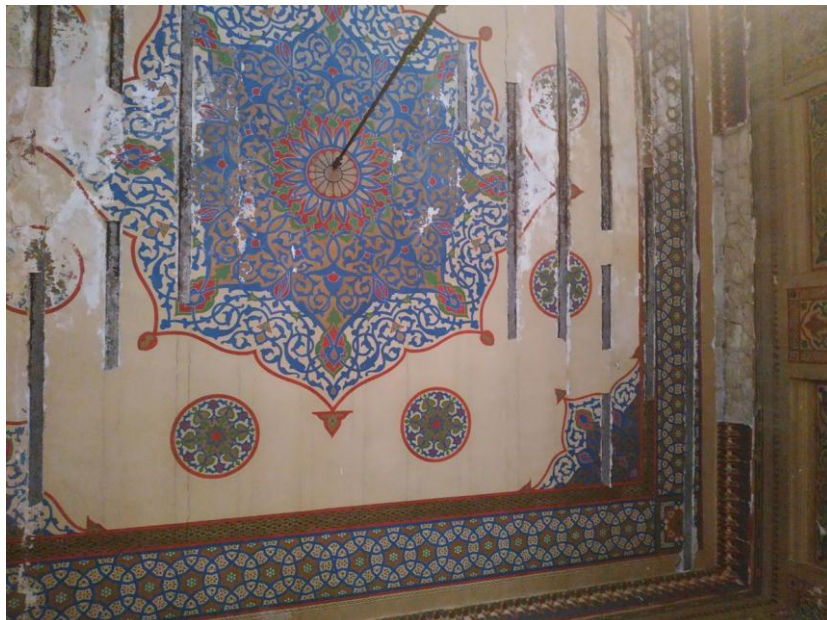

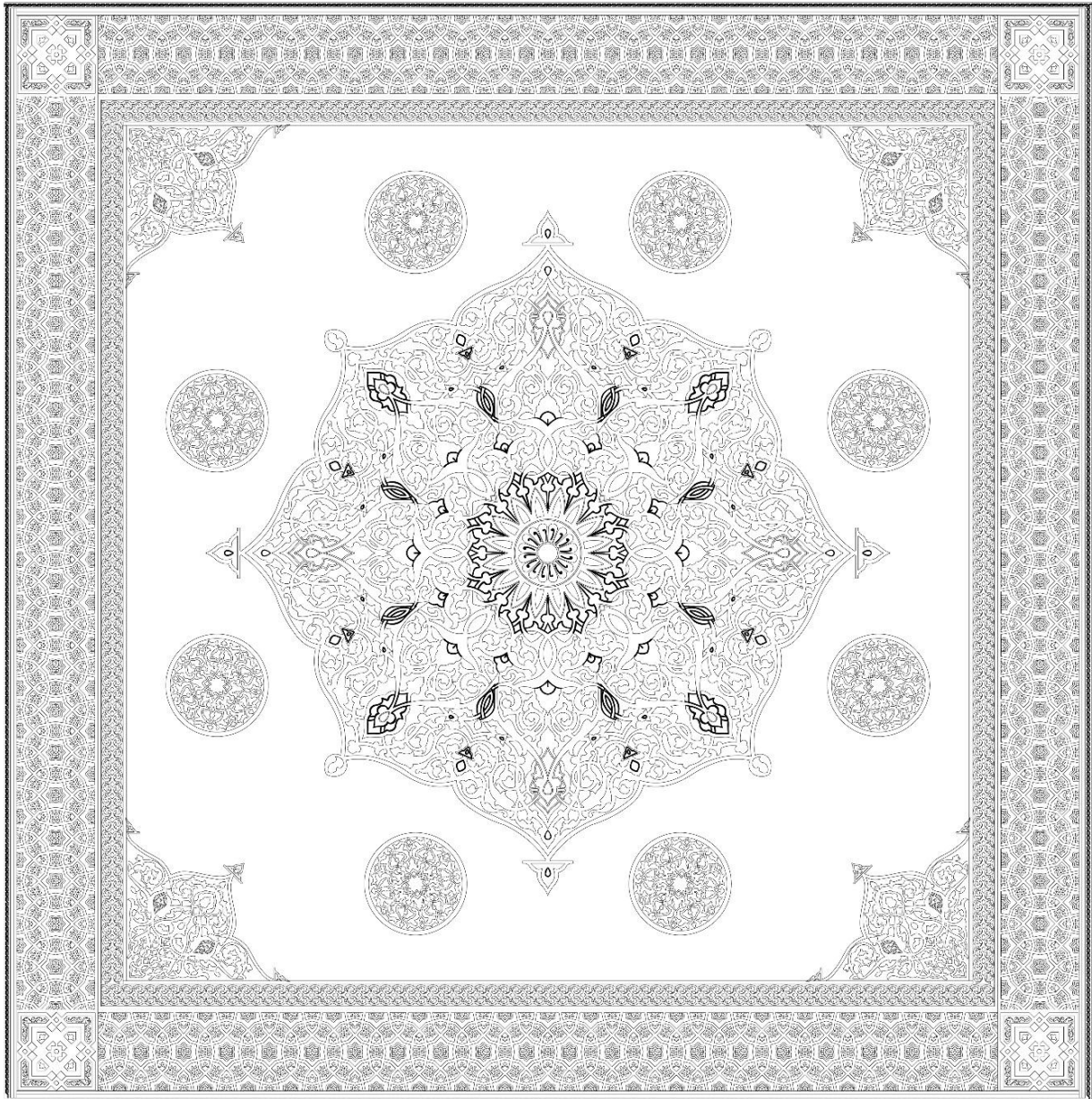Image (4) shows   the ceiling slab damages   in the decoration area

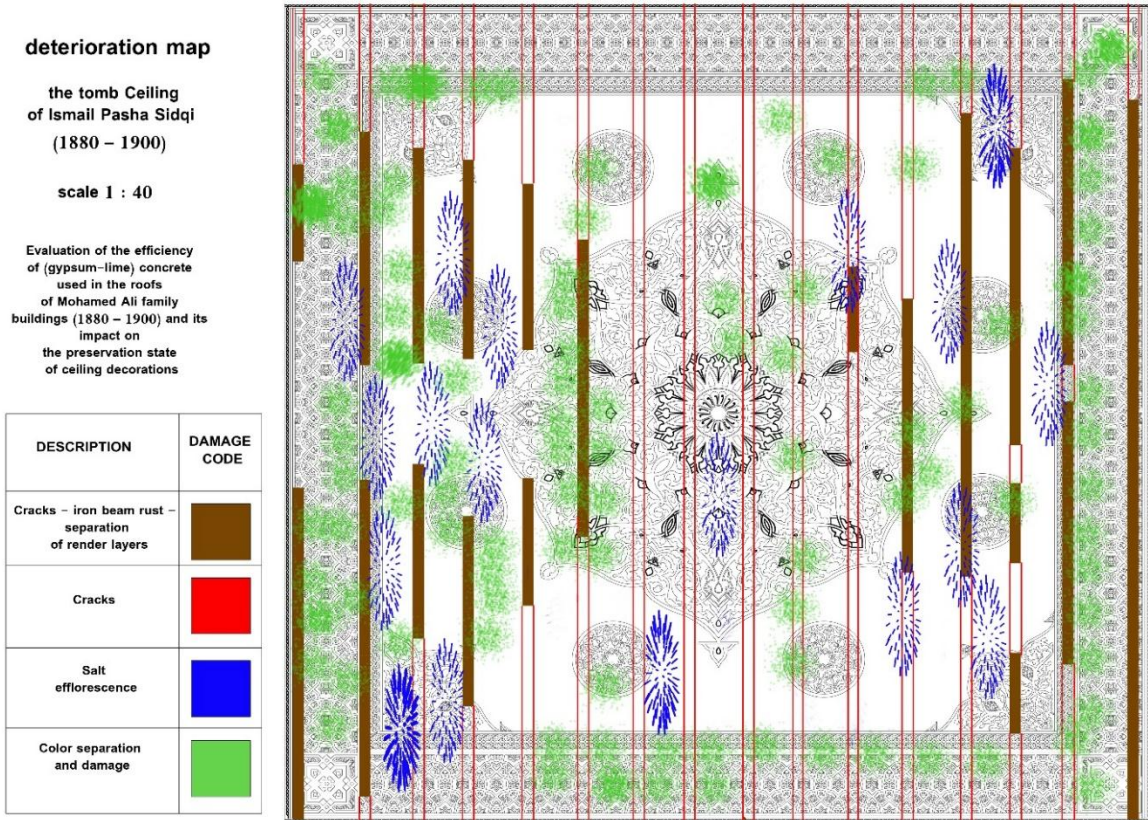Figure (1) shows the design of ceiling decorations

deterioration map

the tomb Ceiling
of Ismail Pasha Sidqi
(1880 – 1900)

scale 1 : 40

Evaluation of the efficiency
of (gypsum–lime) concrete
used in the roofs
of Mohamed Ali family
buildings (1880 – 1900) and its
impact on
the preservation state
of ceiling decorations

DESCRIPTION	DAMAGE CODE
Cracks – iron beam rust – separation of render layers	(brown)
Cracks	(red)
Salt efflorescence	(blue)
Color separation and damage	(green)

Figure (2) shows a map of roof damage

Image (5) shows The spread of rust in iron beams and roof concrete

Image (6) shows peeling of colors, separation of render layers, and the spread of cracks

Image (7) shows render layers damage and the salts efflorescence on
the color layer
Surrounded by the green circle, the salt sample was taken from these
salts efflorescence

Image (8) shows Parts of concrete falling

Image (9) shows Details of the location of the loss
of concrete (the concrete sample that was studied)

II. MATERIALS AND METHODS:

We chose the concrete components conforming to ASTM stander , Hydrated lime conforming to ASTM C207 standard was used ,Gypsum conforming to ASTM C317/C317M-00(2019) was used , Concrete Aggregates conforming to ASTM C 33/C 33M – 08.

Methods.
Analyses the Old damaged concrete binder by X-ray diffraction XRD Device specifications
The qualitative mineralogical analysis was carried out by XRD (powder diffractometer, Philips PW-1050, λ Cu-K α radiation, scanning speed 0.05 $^\circ$ /s). The samples were tested in powder. Scanning electron microscope SEM with EDX used in study Device specifications Scanning electron microscope / FEI Quanta 3D 200i , Edx / thermofisher pathfinder Operated under conditions of low vacuum for acceleration voltage 20.0 ~ 30.0 kv using Large field detector with working distance 15 ~17 mm.
 AG-X Autography Use for mechanical tests Device specifications Type: table- top type Origin: Shimadzu Japan.

Study of the components of the Old damaged concrete.
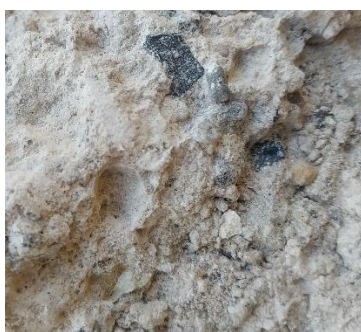

Image (10) of a sample of fallen concrete

Image (11) detailing the components of concrete, showing a white binder, black fillers, and small aggregate of limestone and sand.

Image (12) of the layers of render and colors on the concrete sample

1- The study sample weighed 1 kg of concrete fallen parts.
2- Large fillers of 1-2.5 cm are separated and weighed.
3- The rest of the sample components are weighed and part of them is used for X-ray diffraction analysis.
4- A small fragment of large fillers 1-2.5 cm in size is taken and examined under a scanning electron microscope SEM with EDX.
5- A small fragment of the small fillers is taken and examined under a scanning electron microscope SEM with EDX.
6- The components are defined and their weight percentage is calculated Relative to the The original sample (1 kg weight).

First: Separate the large fillers (1-2.5 cm) in size, weigh them and give a value of 301 g   Relative to the The original sample (1 kg weight)..
Second: A sample is taken from the 700 grams remaining and analyzed by X-ray diffraction to identify the binder of the concrete.

An X-ray diffraction analysis was performed for the sample in powder form after grinding and   separating the large fillers. The sample here expresses the remaining weight after separating the large fillers, which is 700 grams remaining of the total sample weight (1000 g). the analysis shows the presence of gypsum 43.6%, It is considered

The major binding material in the sample was added to lime 24.1%, and the presence of small-sized fillers (sand and dolomite stone) 13.6% for sand and 18.7% for the dolomite. Figure (3)
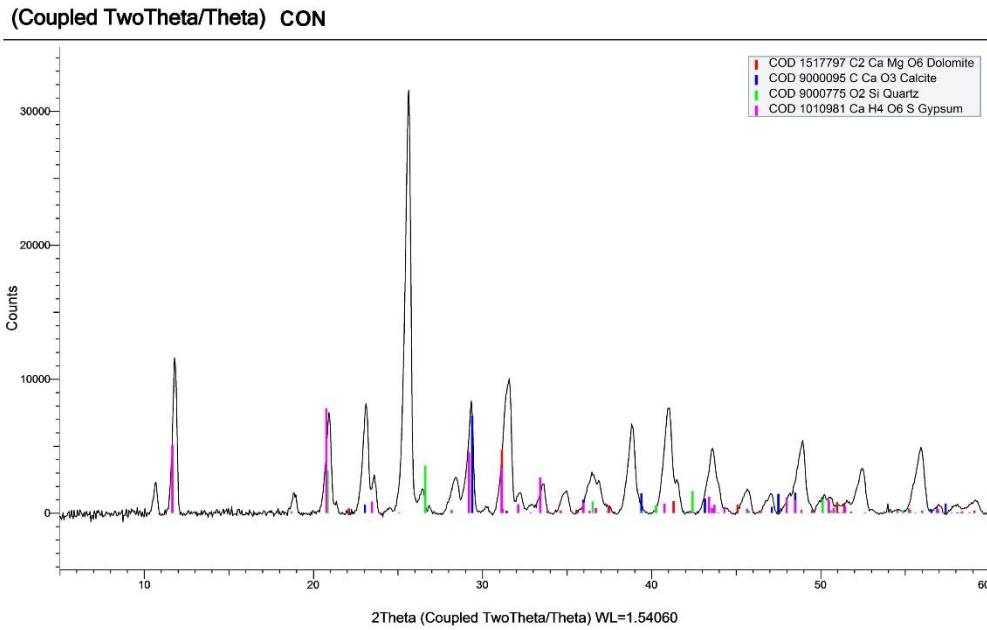
Sample CON

Figure (3) shows the X-ray diffraction pattern of the sample CON
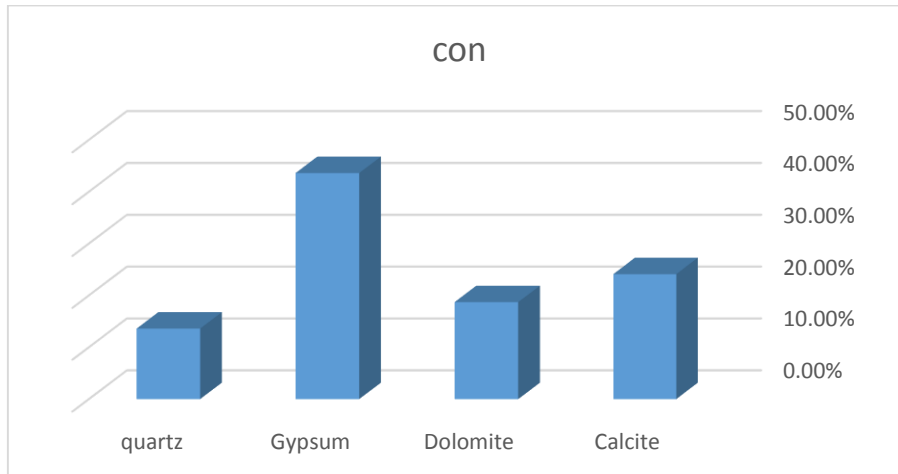

Figure (4) shows the percentages of minerals that consist the sample CON

Table (1) shows the percentages of minerals that consist the sample CON

CON		
Mineral	chemical composition	ratio %
Calcite	$Ca CO_3$	24.1%
Dolomite	$CaMg(CO_3)_2$	18.7%
Gypsum	$CaSO_4 \cdot 2H_2O$	43.6%
quartz	SiO_2	13.6%

Sample Salt

The presence of salt exceeding 92% and the salt efflorescence caused the damage to the render layer, the displacement of the components of the render happened with the salt efflorescence in the outer surface of

render , the disintegration and damage of render layer in the lower part of celling happened due to the periodicity of salt efflorescence Which occurs because the proximity of water sources . Calcite presence confirms that the render is calcareous. Figure (5)
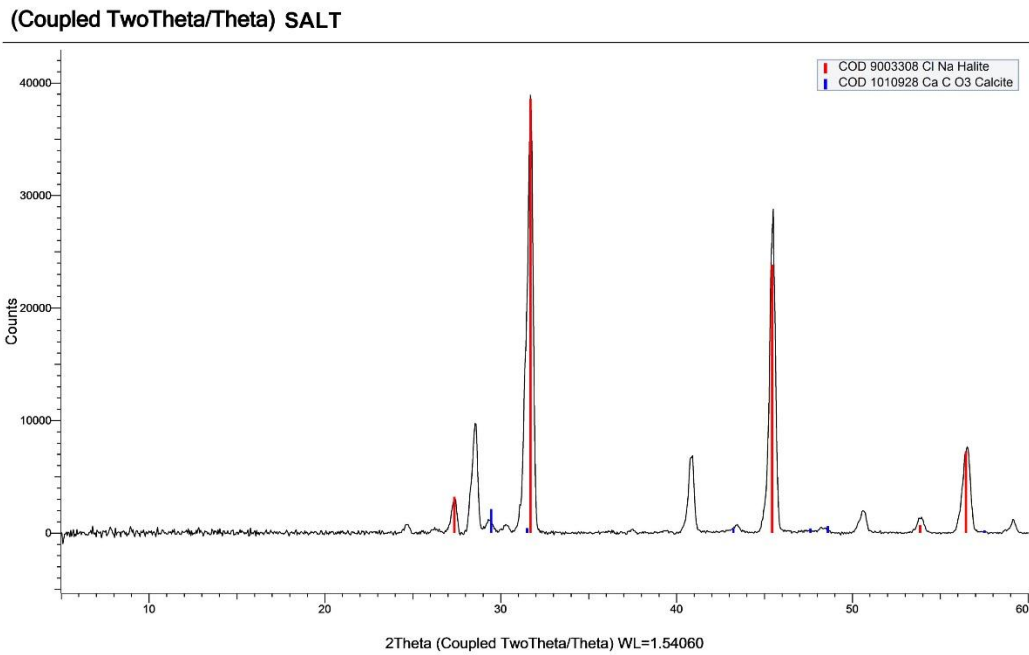

Figure (5) shows the X-ray diffraction pattern of the sample SALT

Figure (6) shows the percentages of minerals that consist the sample SALT

Table (2) shows the percentages of minerals that consist the sample SALT

SALT		
Mineral	chemical composition	ratio %
Halite	Na CL	92.4%
Calcite	Ca CO$_3$	7.6 %

Third: **Examine the fillers under the scanning electron microscope SEM with   EDX unit**
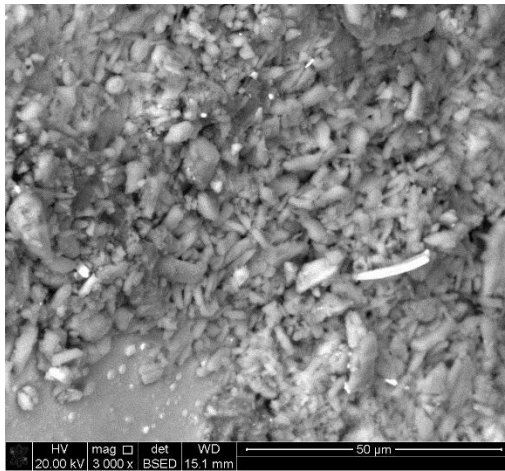
1- Large fillers (1-2.5) cm in size

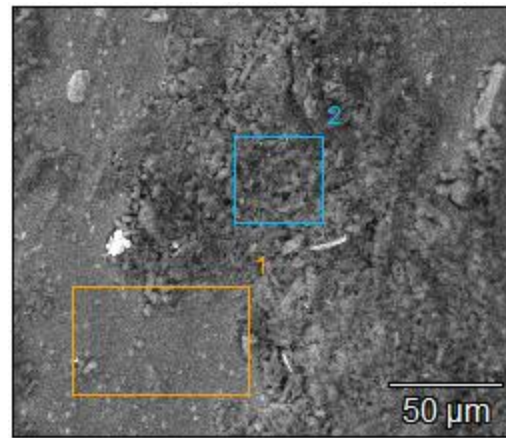Image (13) shows the surface morphology of the filler and shows the surface roughness

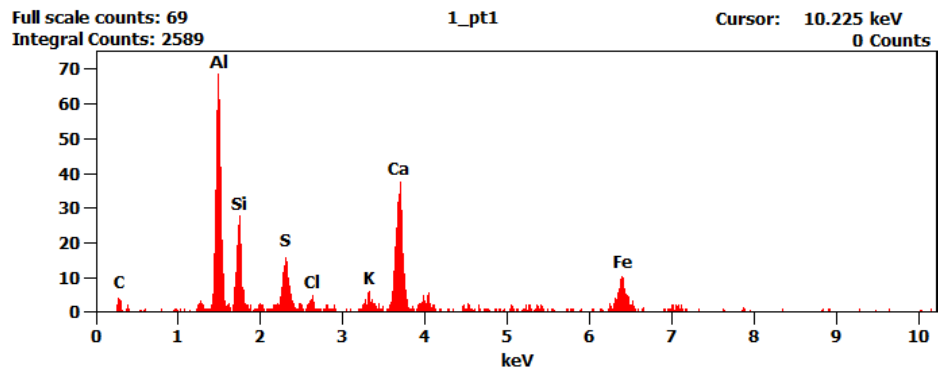Image (14) shows the locations of EDX analysis areas

Figure (7) shows the Edx pattern of the Large fillers sample

Table (3) shows the percentages of Large fillers elements

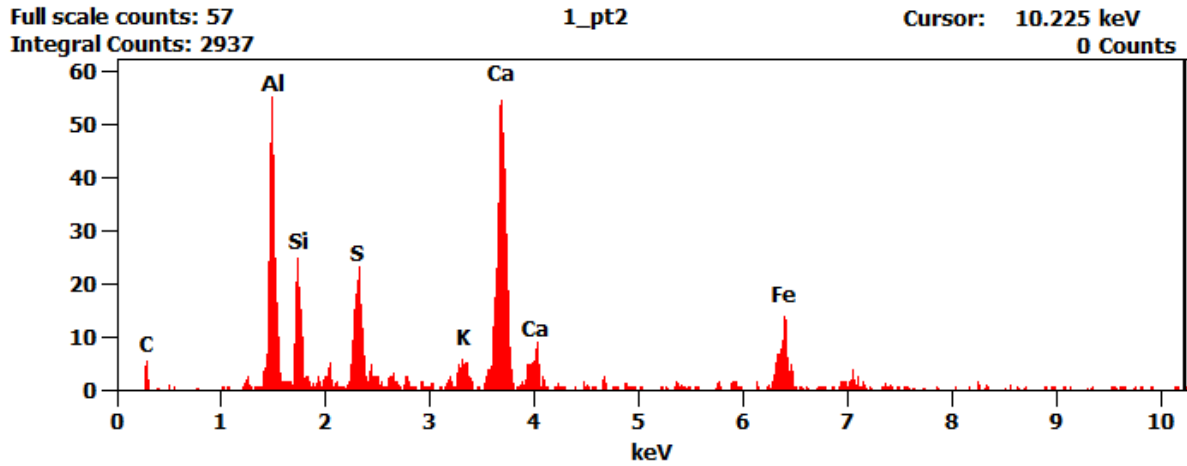|	C	Al	Si	S	Cl	K	Ca	Fe
1_pt1	7.812	23.037	10.649	7.987	1.908	2.679	24.830	21.097
1_pt2	6.781	16.707	8.681	9.857		3.054	33.753	21.167

Figure (8) shows the Edx pattern of the Large fillers sample

Table (4) shows the percentages of large fillers elements

	C	Al	Si	S	Cl	K	Ca	Fe
1_pt1	20.000	26.254	11.659	7.660	1.655	2.107	19.049	11.616
1_pt2	18.215	19.977	9.971	9.919		2.520	27.169	12.228

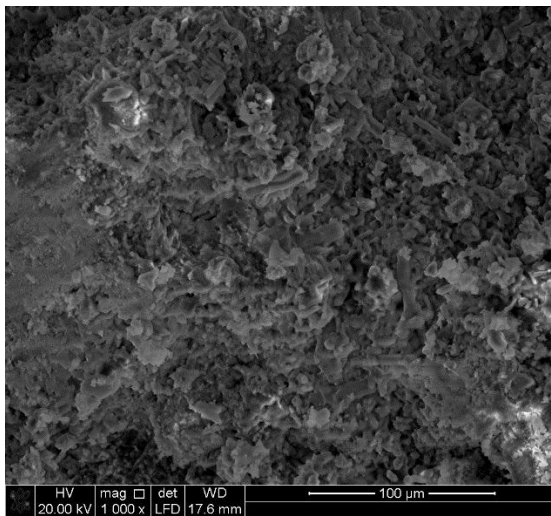**2- Small sized fillers (crushed stone)**

Image (15) shows the filler surface morphology and shows the surface roughness and the presence of salt crystals on the top of the surface Nested with calcite crystals
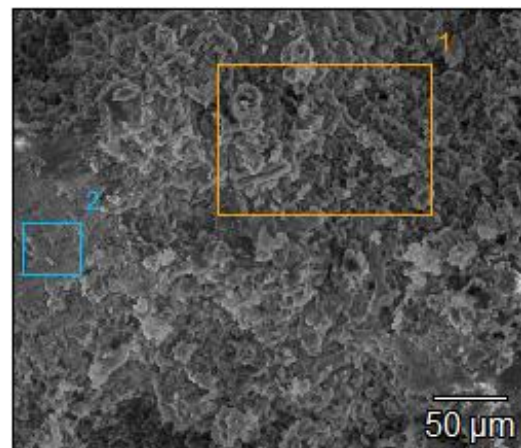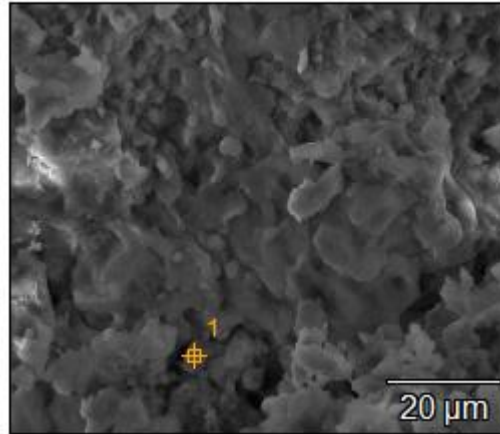
Image (16) shows the locations of EDX analysis areas

2b

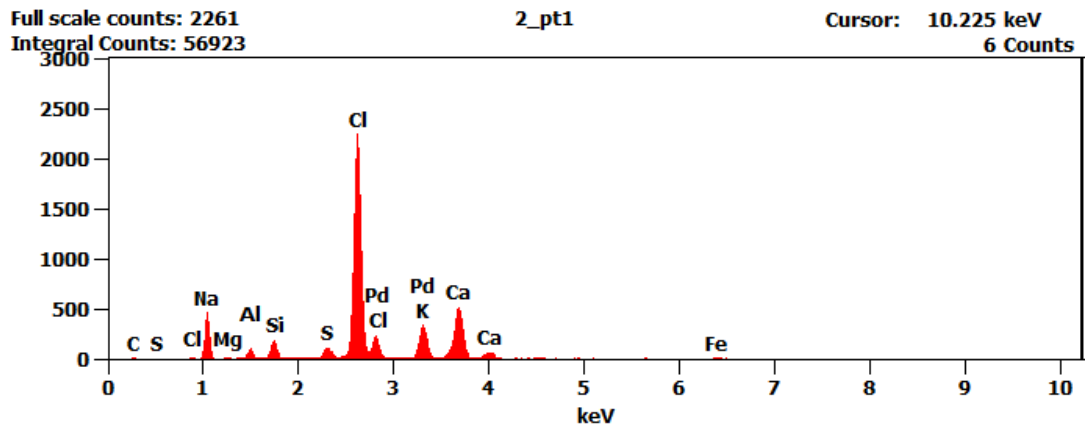Image (17) shows the locations of EDX analysis point

Figure (9) shows the Edx pattern of the Small sized fillers sample (area)

Table (5) shows the percentages of Small sized fillers (crushed stone) elements

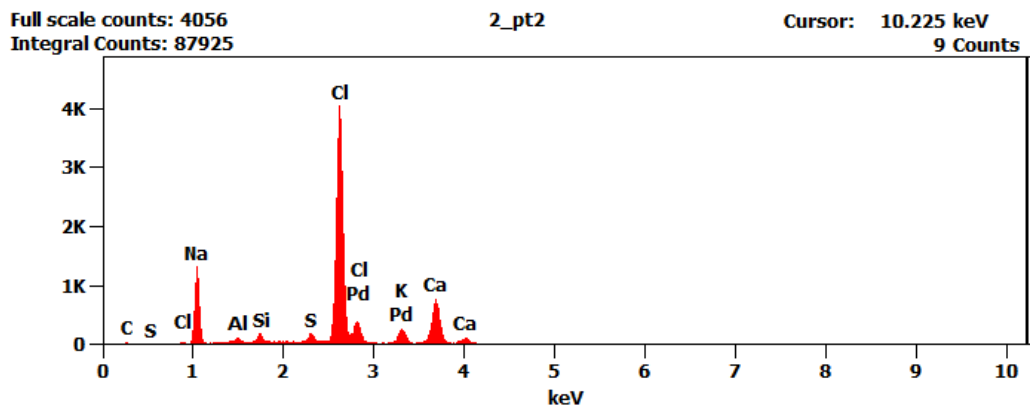|	C	Na	Mg	Al	Si	S	Cl	K	Ca	Fe	Pd
2_pt1	2.833	9.255	0.077	1.615	3.066	2.370	48.289	10.860	20.226	1.409	0.000
2_pt2	3.405	15.823		0.692	1.336	1.908	53.471	5.351	18.014		0.000

Figure (10) shows the Edx pattern of the Small sized fillers sample (area)

Table (6) shows the percentages of Small sized fillers (crushed stone) elements

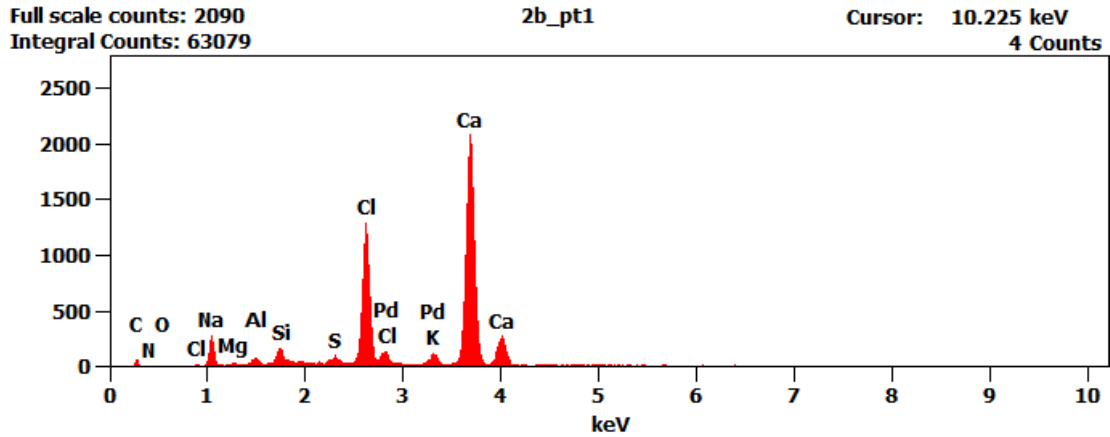|	C	Na	Mg	Al	Si	S	Cl	K	Ca	Fe	Pd
2_pt1	7.723	13.180	0.104	1.960	3.574	2.420	44.596	9.094	16.523	0.826	0.000
2_pt2	8.862	21.515		0.801	1.487	1.860	47.147	4.278	14.050		0.000

Figure (11) shows the Edx pattern of the Small sized fillers sample (point)

Table (7) shows the percentages of Small sized fillers (crushed stone) elements

	C	N	O	Na	Mg	Al	Si	S	Cl	K	Ca	Pd
2b_pt1	4.038	4.107	1.597	5.069	0.167	0.649	1.751	1.090	21.431	2.163	57.937	0.000

According to the result of separating and analyzing the components of the sample weighing 1000 g, the components of concrete are as follows (300 g of basalt size 1-2.5 cm + 305 g of gypsum + 169 g of lime + 131 g of crushed dolomite stone + 95 g of sand). The test samples were constructed in the following proportions (3 parts Basalt gravel + 3 parts gypsum + 1.75 parts lime + 1.25 parts crushed dolomite + 1 part sand)

Casting and testing

Three concrete specimens were casted for each size considered

Table (8) shows the specimens were casted

Sample code	Dimension	Condition
Sample 1	5cm ^{3}	Fresh sample
Sample 2	5cm ^{3}	salt-aged sample
Sample 3	10cm ^{3}	Fresh sample
Sample 4	10 ×14.5 ×50	Fresh sample mock-up

First: casting samples, measure physical properties and compression & bending test

A- Concrete Raw materials processing

| Image (18) shows crushed dolomite | Image (19) shows Basalt gravel | Image (20) shows sand | Image (21) shows gypsum and lime |

B- Casting the simulating model (mock-up) and filling concrete

Image (22) shows the insulation of a 5 cm^3 sample casting mold

Image (23) shows the insulation of a 10 cm^3 sample casting mold

Picture (24) shows preparing molds for casting

Image (25) shows the samples after pouring into the molds

Image (26) shows the completion of casting the mock-up

Image (27) shows the completion of casting the mock-up

Image (28) shows the completion of casting the sample 10 cm3 , 5 cm3

Second - estimate Concrete physical properties

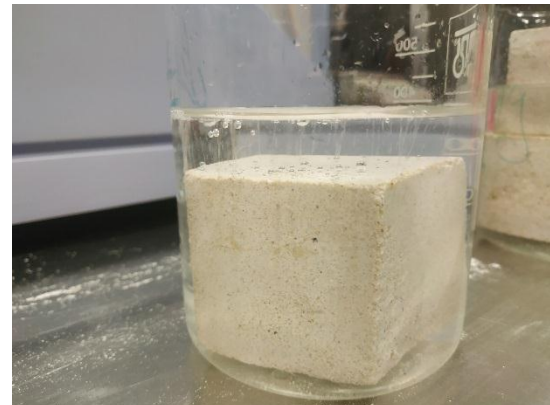Image (29) shows Weighing samples to estimate their physical properties

Image (30) shows Soaking samples in distilled water to estimate physical properties

Table (9) shows Concrete physical properties values

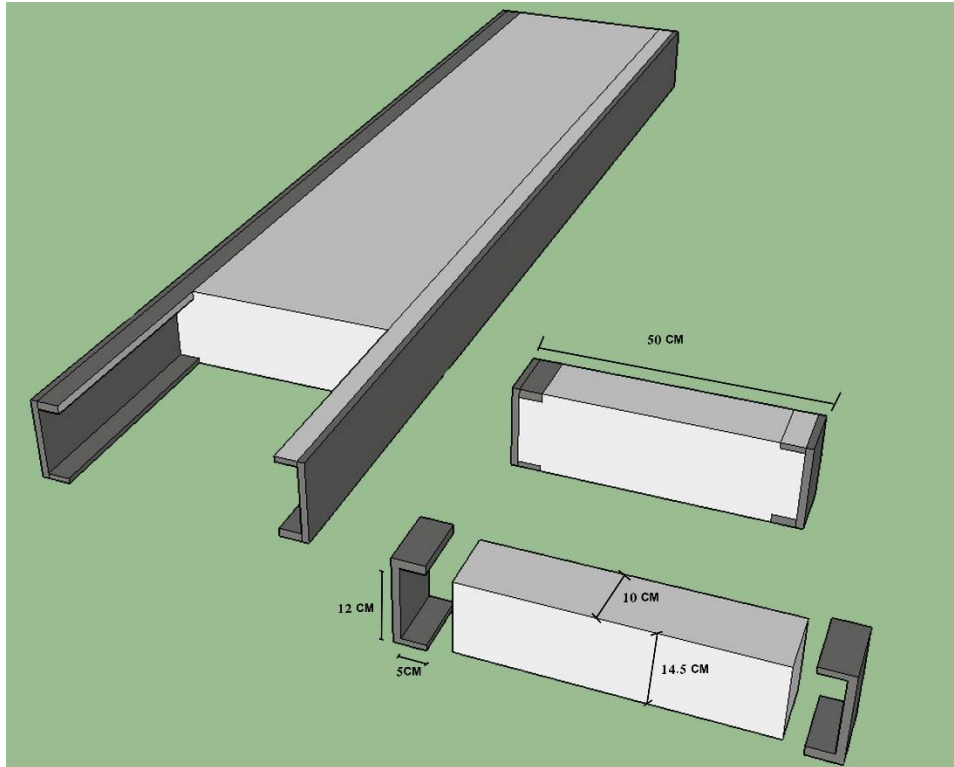| sample	Dry weight g	Wet weight g	Volume cm^3	Density g/cm^3	porosity %	Water absorption %
cube 1	184.56	228.39	125	1.47	35	23
cube 2	188.80	231.14	125	1.51	33	22
cube 3	189.07	234.09	125	1.51	36	23
average	187.49	231.20		1.49	34	23

Figure (12) shows the concrete mock-up and its dimensions

Third: Compression and bending test of samples

Samples with size 5 cm3 and 10 cm3 were prepared from the concrete mix, and a compression test done for the samples before and after aging. The bending test was carried out on the simulation model (mock-up) of the roof slab, with dimensions in the Figure (12) 10 * 14.5. *50 Tests were done after 180 days to ensure complete carbonization of lime occurred in the samples .

Salt aging of the samples was carried out by soaking in a 5% salt solution (sodium chloride) for 1 hour, then drying at room temperature, then repeating the soaking process for 10 cycles. The effect of salt weathering on the load strength of the samples was tested.

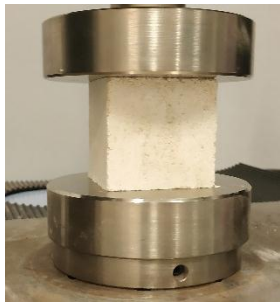Image (31) shows samples and mock-up before testing

Image (32) shows the compression test of cubes Sample1(5 cm3)

Image (33) showing the collapse of the cube Sample1

Image (34) shows the compression test of sample No. 2 (5 cm3) after salt aging and in a wet condition

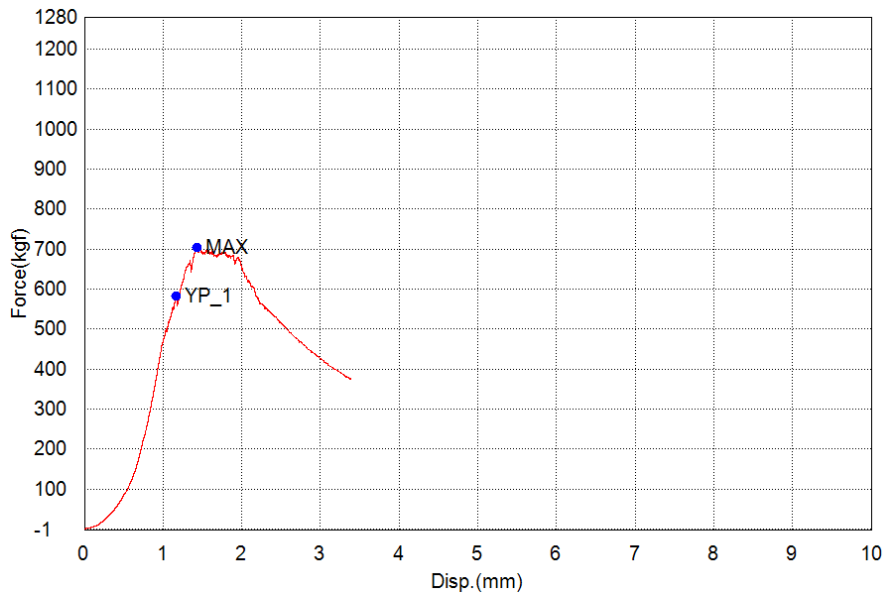Image (35) shows the collapse of sample No. 2 after salt aging and in a wet condition

Figure (13) shows the compressive force until collapse of sample 1

Table (10) shows compressive strength values of Sample 1

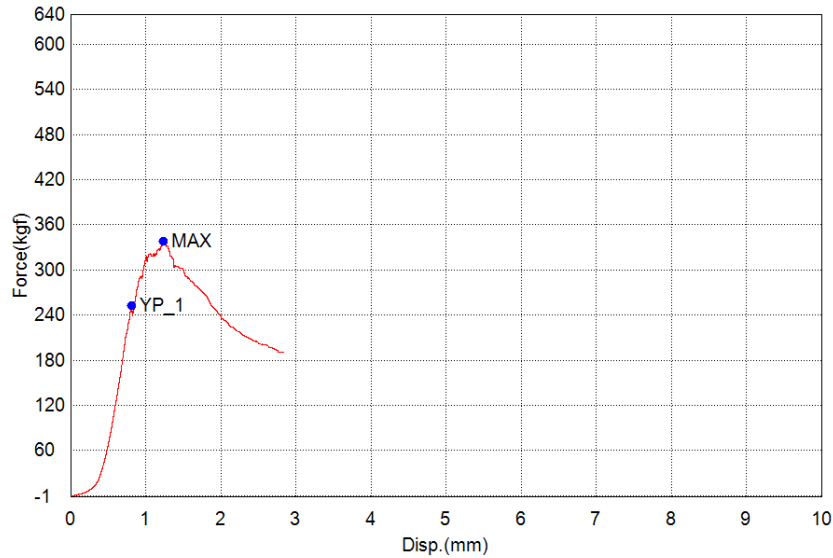| Sample 1							
Speed	No of Batches	Sample size	face area	Break_Stroke Max_Force kgf/ f area	Break_Stroke Max_Force kgf/ cm	YP(%FS)_Force kgf/ f area	Max_Stroke at Entire Areas mm
1mm/min	1	5cm ^{3}	25cm^3	702.736	28.1	581.486	1.43079

Figure (14) shows the compressive force until collapse of sample 2

Table (11) shows compressive strength values of Sample 2

Sample 2							
Speed	No of Batches	Sample size	face area	Break_Stroke Max_Force kgf/ f area	Break_Stroke Max_Force kgf/ cm	YP(%FS)_Force kgf/ f area	Max_Stroke at Entire Areas mm
1mm/min	1	5cm^3	25cm^3	337.841	13.51	253.104	1.24098

The test showed a significant decrease in the sample's load capacity value due to exposure to salt ageing cycles, as the load capacity value reached 52% of the load value for the sample that was not subjected to aging. In addition the sample had some moisture and was not completely dry, which explains the decrease in the strength of the sample.

Here noted that the displacement from the point of load, after which resilience does not occur until collapse, was large compared to the displacement in the dry sample, as it reached 0.44 mm in the sample that was subjected to weathering and 0.25 mm in the sample that was not subjected to aging. This confirms that the sample that was not subjected to aging was

Less resistance during collapse after passing the load after which resilience does not occur. The reason for this is due to the high hydration of the sample, which increased the percentage of flexibility of the sample that was subjected to aging, despite the significant weakness in the loading strength for the sample, which was reduced by half.

Image (36) shows the compression test of cubes Sample 3 (10 cm3)
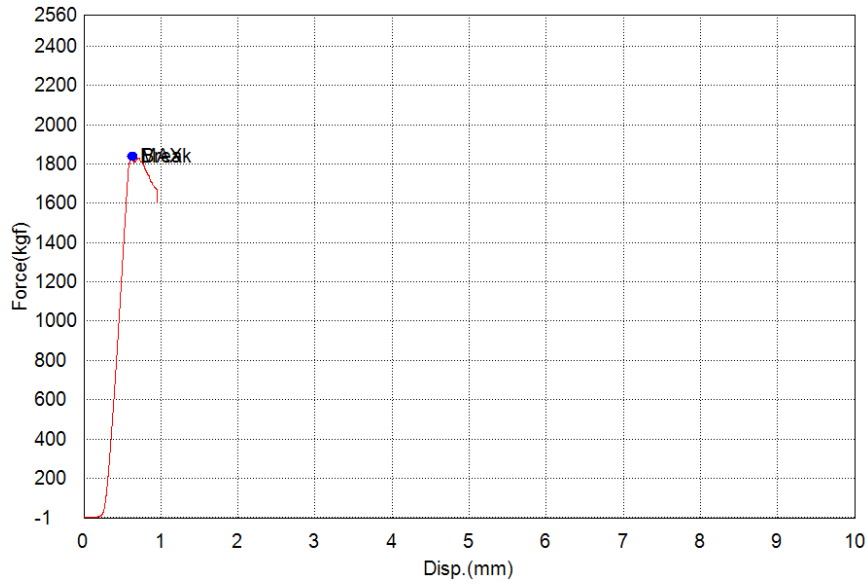
Image (37) showing the collapse of the cube Sample3

Figure (15) shows the compressive force until collapse of sample 3

Table (12) shows compressive strength values of Sample 3

Sample 3						
Speed	No of Batches	Sample size	face area	Break_Stroke Max_Force kgf/ f area	Break_Stroke Max_Force kgf/ cm	YP(%FS)_Force kgf/ f area
5mm/min	1	$10cm^3$	$100cm^3$	1841.54	18.41	00

bending test

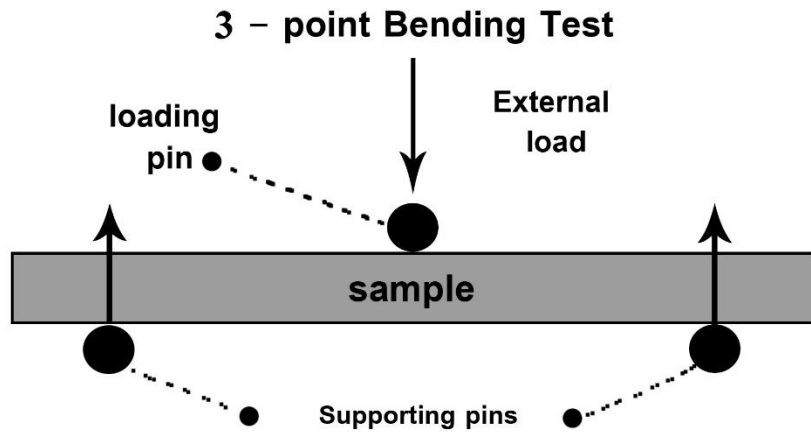Image (38) shows the mock-up being placed on the test device

Figure (16) shows the type of bending test

Image (39) shows supporting pins before testing

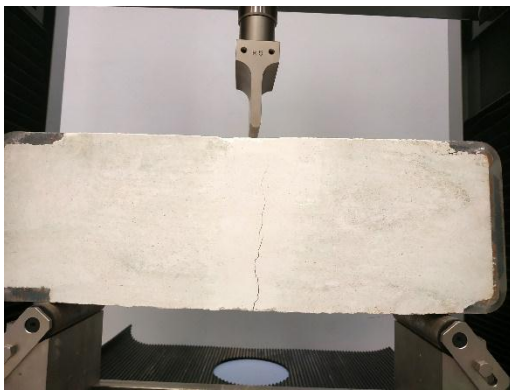Image (40) shows loading pin before testing

Image (41) showing the collapse of the mock-up
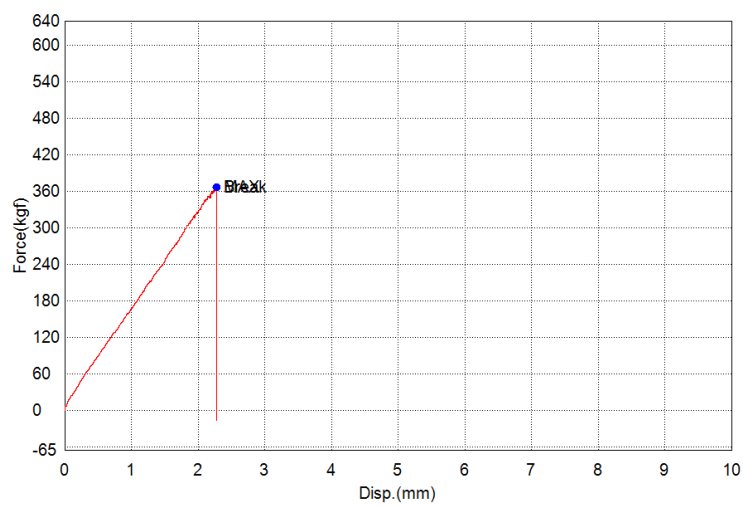

Image (24) showing the collapse of the mock-up

Figure (17) shows the Applied force until collapse of sample 4 (mock-up)

Table (13) shows bending test results of Sample 4

| Sample 4						
Speed	No of Batches	Sample size	face area	Break_Stroke Max_Force kgf/ f area	Break_Stroke Max_Force kgf/ cm	YP(%FS)_Force kgf/ f area
1mm/min	1	10 ×14.5 ×50	450cm^2	366.528	.81	00

Here the fracture occurred directly without a resilience loading point after which it could rebound, this caused by the drying of the tested model.

III. DISCUSSION:

Unreinforced concrete it lasts for 125 years, is a matter that requires explanation, especially the binder components of concrete are weak components and are not used individually for construction purposes. An X-ray diffraction analysis for concrete The analysis shows the presence of gypsum 43.6%, It is considered The major binding material in the sample was added to   lime 24.1%, and the presence of small-sized fillers (sand and crushed dolomite stone -Image (11)) 13.6% for sand and 18.7% for the dolomite. Figure (3,4) Table (1). Large fillers (1-2.5) cm in size were basalt gravel Image (13) Figure (9) Table (5) Basalts are common aphanitic igneous extrusive (volcanic) rocks. Basalts are composed of minute grains of plagioclase feldspar (generally labradorite), pyroxene, olivine, biotite, hornblende and <20% quartz. [6]

Concrete physical properties   was low in density 1.49 g/cm3 and high in porosity 34% and water absorption 23 % Table (9) , which means it was not good concrete. The cracks spread parallel to the path of the steel beams , rusting of iron beams, separation of render layers, peeling of colors, and falling parts of concrete that fills   between the iron beams. Image (4,5,6,7,8,9) Figure (1,2) Despite all this, concrete still remains and performs its function.

The explanation for this is Binders and fillers work together in harmony way , gypsum setting is the opposite of removing water process from raw gypsum, as the paste of gypsum contains about 6.2% water and can easily absorb water and turn into hydrated calcium sulfate again, where its crystals take the needle shape, forming a solid mass. [7]

$CaSO_4. 1\backslash2 H_2O + 1 1\backslash2 H_2O \longrightarrow CaSO_4. 2H_2O$
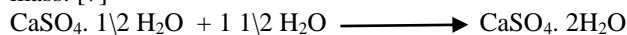
Many types of gypsum were monitored to measure the expansion resulting from hardening during the period from 96 to 120 hours after mixing the mortar. The expansion rate was 0.57% +/- 0.02%, [8] which explains the absence of cracking after hardening.

Air lime depend on exposure to air to harden them, as slaked lime reacts with carbon dioxide (CO2) present in the atmosphere.

$Ca (OH)_2 + CO_2 \longrightarrow CaCO_3 + H_2O$
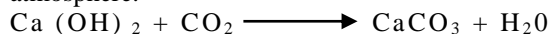
It is clear that during solidification, carbonization and dehydration occur simultaneously, which causes shrinkage in size. [9] In fact Cracks that develop in lime concrete tend to heal themselves, unlike conventional mortar made with Portland cement, The rate of carbonization depends on the grain size of the concrete fillers   , which has the effect of speeding up the carbonization process. [10] In our case study, there is a variety in the size of the filling materials, as there are crushed dolomite and large basalt Gravel, So we can say that we have a Gravel concrete these of course formed with lime as the matrix.

it has been observed that HSSCCs (High Strength Self-Compacting Concrete) with high strength and durability properties can be produced by using basalt   aggregates at rates of 25 % to 100 % . [11] Therefore, basalt is a very suitable filler for lime and gypsum, This gives the concrete a reasonable durability. [12]

Concrete as known, is relatively strong in compression and weak in tension. In reinforced concrete members, little dependence is placed on the tensile strength of concrete since steel reinforcing bars, are provided to resist all tensile forces. It has been argued that the flexural strength property of concrete is important particularly when the concrete structure has no steel reinforcement. So the Unreinforced concrete consider a brittle materials, the bending test is often more suitable than the tensile test, because the materials are subjected to bending stress only [13] like our case. Here the fracture occurred directly without a resilience loading point after which it could rebound, this caused by the drying of the tested model , Figure (17) Table (13) despite of achieved a reasonable value of force up to 366.528 kgf/ f area .

It must be noted that the   compressive strength test for samples had a resilience point, especially the sample that had been subjected to aging and had some amount of moisture, Sample 1, 2 Figure (13 ,14) Table (10 ,11)

The test showed a significant decrease in the sample's load capacity value due to exposure to salt ageing cycles, as the load capacity value reached 52% of the load value for the sample that was not subjected to aging. In addition the sample had some moisture and was not completely dry, which explains the decrease in the strength of the sample.

Here noted that the displacement from the point of load, after which resilience does not occur until collapse, was large compared to the displacement in the dry sample, as it reached 0.44 mm in the sample that was subjected to weathering and 0.25 mm in the sample that was not subjected to aging. This confirms that the sample that was not subjected to aging was

Less resistance during collapse after passing the load after which resilience does not occur. The reason for this is due to the high hydration of the sample, which increased the percentage of flexibility of the sample that was subjected to aging, despite the significant weakness in the loading strength for the sample, which was reduced by half. This weakness came   as a result of the salt crystallization on the edges of the filling materials as Salt is found on the surface of aggregate materials mixed with the binders. [14] Where you notice the presence of chlorine, sodium, and potassium ions that make up halite and Sylvite salts Image (15) Table (7) Figure (18)

Figure (18) shows the locations of salt crystallization within the concrete matrix
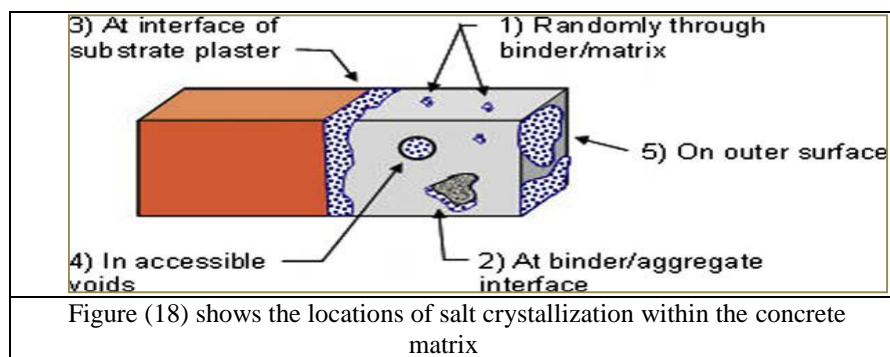
IV.   CONCLUSION:

• Unreinforced concrete (gypsum-lime) lasts for 125 years due to Durability of binders, gypsum and lime and The variety of filling materials and their different sizes.

• Gypsum can be used for construction purposes if water is prevented from reaching it.

• Gypsum expands during hardening The expansion rate was 0.57% +/- 0.02%, which explains the absence of (gypsum-lime) cracking after hardening.

• Cracks that develop in lime concrete tend to heal themselves.

• Unreinforced concrete (gypsum-lime) has a variety in the size of the filling materials, as there are crushed dolomite and large basalt Gravel, So we can say that we have a Gravel concrete these of course formed with lime as the matrix. And speeding up the lime carbonization process .

• Using basalt aggregates Increases the durability of concrete (gypsum-lime) .

• due to the high hydration of the concrete (gypsum-lime) that was subjected to aging its   flexibility increased .

• The high hydration of the concrete (gypsum-lime) led to weakness in the loading strength, which was reduced by half.

• The salt crystallization on the edges of the filling materials It has a strong effect on weakening the mechanical strength of concrete.

• The celling must be insulated and prevent any water reaching to the concrete (gypsum-lime) to preserve it.

REFERENCES:

[1]. Suheir Helmy, (2003.) .The Family of Muhammad Ali. Egyptian General Book Authority, p 55
[2]. Egyptian Gazette, Issue 74, March 29, 2023. p 6
[3]. Muhammad Thabet,(2020) .Civil and educational Buildings in   Muharram Bek district in   Alexandria city , era of the Muhammad Ali family (an archaeological and architectural study). Ph.D , Faculty of Arts, Helwan University, Egypt , p. 39
[4]. Rainer . l, Rivera . A, (2004) .The conservation of decorated surfaces on Earthen Architecture. The getty conservation institute los Angeles   , p 16

[5]. Ridout .V (2008) .Moisture Monitoring in Earthen Structures Earthen Architecture Conservation . The Getty Conservation Institute, Los Angeles, p28

[6]. Xingfen Chen , Yunsheng Zhang , David Hui , Meirong Chen , Zhishen Wu (2017) . Study of melting properties of basalt based on their mineral components. Composites Part B Engineering, Volume 116, P 53-60

[7]. Coburn.A , Dudley.E , Spence.P (1989) .Gypsum plaster its manufacture and use . intermediate technology publications ,p4

[8]. Konstantinos X. Michalakis, DDS, MSc, PhD,a Athanasios Stratos, DDS,b Hiroshi Hirayama, DDS, DMD, MS,c Argiris L. Pissiotis, DDS, MS, PhD,d and Foteini Touloumi, DDSe (2009) . Delayed setting and hygroscopic linear expansion of three gypsum products used for cast articulation. Aristotle University ,School of Dentistry, Thessaloniki, Greece, p10

[9]. Brimblecombe .P, (2002) .The effect of air pollution on the built environment . Air pollution Reviews _ Vol. 2 University of east Anglia , UK,p113

[10]. Turki .A. El, Carter . M.A, Wilson. M.A, Ball. R.J, Allen. G.C (2009) . A microbalance study of the effects of hydraulicity and sand grain size on carbonation of lime and cement. Construction and Building Materials 23, p 1423–1428

[11]. Ahmet Raif Boğa , Ahmet Ferdi Şenol (2023).The effect of waste marble and basalt aggregates on the fresh and hardened properties of high strength self-compacting concrete. Construction and Building Materials ,Volume 363 , p 144-154

[12].   Anthony W. et al. (2015) .The Effect of Maximum Coarse Aggregate Size on the Compressive Strength of Concrete Produced in Ghana. Civil and Environmental Research, Vol.7, No.5, p 36.

[13]. Awodiji Gloria etal (2017) . Flexural and Split Tensile Strength Properties of Lime Cement Concrete. Civil and Environmental Research Vol.9, No.3, p56

[14]. Lubelli, Barbara & de Rooij, Mario (2009) .NaCl crystallization in restoration plasters. Construction and Building Materials Volume 23, Issue 5, P 1736-1742.